Linear and nonlinear optical properties of Au/SiO_2 nanocomposite prepared by P123

Jingyue Fang (方靖岳)*, Shiqiao Qin (秦石乔), Xueao Zhang (张学骜), and Shengli Chang (常胜利)

School of Science, National University of Defense Technology, Changsha 410073, China

**Corresponding author: fjy_nudt@yahoo.com.cn*

Received August 11, 2011; accepted September 9, 2011; posted online November 1, 2011

Mesoporous silica thin films loaded with gold nanoparticles are synthesized in the presence of $EO_{20}PO_{70}EO_{20}$ (P123). Transmission electron microscope images show that the matrix of the nanocomposite is an ordered porous structure with a two-dimensional hexagonal phase. The wide-angle X-ray diffraction pattern implies that the nanocomposite contains gold crystals. These metallic nanoparticle-embedded solid thin films show some linear and nonlinear optical properties due to their special structure and composition. Gold nanoparticles bring about surface plasmon resonance, and an absorption peak stemming from this effect has been observed. The linear absorption property is analyzed by a quantum mechanism, and the results show that it is influenced by the size and volume fraction of gold nanoparticles. Furthermore, it shows an obviously clear nonlinear optical property measured by the z-scan technique. The magnitude of the nonlinear refractive index of the nanocomposite is estimated to be about 10^{-10} cm^2/W.

OCIS codes: 160.4330, 190.4720, 240.6680, 310.6860.

doi: 10.3788/COL201210.031601.

Mesoporous silica thin film (MSTF) has been widely studied because of its special structure: it has highly ordered nanoscale pores and its surface area is much larger than bulk materials. Furthermore, the pore size of MSTF can be regulated by adjusting the preparation conditions, which makes it suitable as a template to assemble other nanomaterials. Metallic nanoparticle (MNP) possesses novel optoelectronic properties, and the MSTF provides one of the means to synthesize MNPs and get the nanocomposite of MNP-embedded silica thin films. If the MNPs can be loaded in each pore of the MSTF, MNPs array can be obtained in silica thin films. In addition, the resultant MNPs@MSTF nanocomposite is compatible with conventional Si fabrication technology. Moreover, this technology can fabricate single-electron tunneling devices using the MNPs@MSTF nanocomposite[1,2]. They are expected to surpass the limits of conventional silicon devices with ultra-low power and scalability down to the sub-nanometer regime.

We have reported the synthesis of MSTF incorporated with gold nanoparticles (GNPs)[3]; in this letter, we mainly discuss its optical property. As the surface plasma resonance (SPR) of GNPs, the nanocomposite displays some linear optical properties, such that the absorption peak can be controlled by the MSTF structure, as well as the size and volume fraction of GNPs[4−6]. Within the framework of the Drude dispersion relation, the SPR absorption, including that of particles smaller than 10 nm, can be successfully explained with the Maxwell-Garnett (MG) theory. If the GNPs are so small that the conduction band breaks into discrete levels, the Drude expression may no longer be valid and should be replaced by a quantum mechanical model[7]. We use the quantum mechanical model to analyze how the size and volume fraction of GNPs influence the optical property of the GNPs@MSTF nanocomposite. Nonlinear optical property is another important trait of this nanocomposite, and we get the third nonlinear refractive index by the z-scan technique[8].

The synthesis of MSTFs was carried out according to the template-assisted evaporation-induced self-assembly procedure in the presence of surfactant template $EO_{20}PO_{70}EO_{20}$ (P123) under acidic conditions. The final reactant molar ratio was tetraethoxysilane (TEOS): 3-aminopropyltriethoxysilane (APTES): C_2H_5OH: HCl: H_2O: P123 = 0.9: 0.1: 20: 0.15: 5: 0.01. More details can be found in our previous work[3]. Using $HAuCl_4$ as the gold precursor, GNPs were incorporated in the mesopores of MSTFs by means of neutralization and reduction reactions. GNPs@MSTF samples with different reaction time of 2, 6, and 10 h were produced.

Transmission electron microscope (TEM) images were recorded to observe the surface of MSTFs using FEI Tecnai G^2 20 S-Twin apparatus at an accelerating voltage of 200 kV. X-ray diffraction (XRD) patterns were obtained using a Rigaku D/MAX2200 diffractometer featuring Cu Kα radiation (λ = 0.15418 nm) at 40 kV and 200 mA. Ultraviolet-visible (UV-VIS) absorption spectra were recorded on a spectrophotometer (U–4100, Hitach, Japan) with 2-nm resolution using air as reference. Moreover, z-scan measurements were performed using a Ti:sapphire laser (Mai Tai HP, CA, USA) operated at a repetition rate of 80 MHz in TEM_{00} mode with an average power of about 2 W.

Figures 1(a) and (b) demonstrate the striped channels and ringent hexagonal pores, respectively, implying that MSTF possesses a highly ordered porous structure with a two-dimensional (2D) hexagonal phase.

The wide-angle XRD pattern of Fig. 2 confirms that well-crystallized GNPs are incorporated in the matrix of MSTF since the intensity peak at about 38° can be indexed to the (111) reflections of the face-centered cubic (FCC) gold. The inset in Fig. 2 shows the high-resolution TEM (HRTEM) image of a single 8.5-nm-diameter GNP (the period of the striped channels is about 0.24 nm). This verifies that the GNP is well crystallized and that the pore of MSTF confines its size.

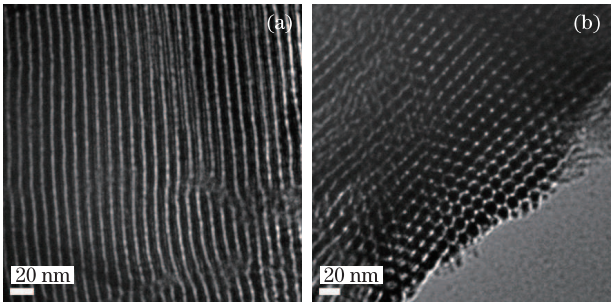

Fig. 1. TEM images of MSTFs prepared by the surfactant P123. (a) The striped channels and (b) ringent hexagonal pores.

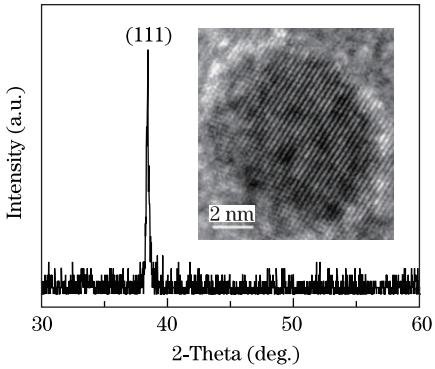

Fig. 2. Wide-angle XRD pattern of a GNPs@MSTF composite film with a six-hour reaction; the inset is a HRTEM image of a single GNP.

Based from the TEM and XRD characterizations, the nanocomposite has some features: (1) the matrix is a porous structure and its dielectric constant would be changed by the pore size and pore arrangement; (2) GNPs are embedded in the matrix and the dielectric function of the nanocomposite may be influenced by the GNPs' size and volume fraction controlled by reaction conditions; (3) GNPs are small in size in the MSTF pores, and the nanocomposite may display the third-order optical nonlinearity due to the quantum size and interfacial effects.

An absorption spectrum of a GNPs@MSTF composite film (six-hour reaction time) shown in Fig. 3(a) exhibits that the absorption peak is located at about 575 nm, which is caused by the SPR of the embedded GNPs. Experimental results shown in Fig. 3(b) indicate that along with the increase in reaction time (neutralization reaction between the -NH_4 and -$AuCl_4$ groups), the particle size of GNPs in the resultant nanocomposite also increases. The embedded TEM images of Fig. 3(b) show dispersed GNPs released from the nanocomposites with different reaction time. The size ranges are 4.3−10, 6.0−12.0, and 6.5−13.6 nm, and the average sizes are 7.4, 8.0, and 8.7 nm with reaction time of 2, 6, and 10 h, respectively. Furthermore, the absorption property changes regularly, such that the absorption peak moves to longer wavelength and the peak intensity is enhanced. To analyze how the size and shape of GNPs affect the absorption peak position and intensity of the GNPs@MSTF nanocomposite, the Drude dispersion model and the GM theory are employed in this letter for simulations, which are shown in Fig. 4[4,5]. The results are calculated in the assumption that the diameter and the wall thickness of the mesopores are 7 and 5 nm (a fixed MSTF structure), respectively, with a fixed filling ratio of 0.7 (70% of the pores are filled with GNPs). The size ratio (lateral axis of the GNP to the pore diameter) mainly influences the absorption intensity, whereas the aspect ratio (vertical axis to the lateral axis of the GNP) affects both the absorption peak location and intensity. Thus, the red shift and intensity enhancement of Fig. 3(b) are probably due to the increase in size ratio and decrease in aspect ratio of the GNPs. In conclusion, the confirmation of the nanopores probably causes the shape of the embedded GNPs to change from globe to prolate spheroid with increasing reaction time. Furthermore, we tentatively assume that the extinction property of the GNPs@MSTF nanocomposite can be controlled by regulating the neutralization reaction time.

The dielectric function of MNPs can be described by the Drude dispersion model[9,10]. For small particles where the conduction band breaks up into discrete levels, Genzel *et al.*[7] has given a more realistic, quantum-mechanically derived dielectric function. The model is that of free electrons in a cubic potential well with infinite sides, which can be applied to very small particles (less than 20 nm). To make a comparison, we introduce this model in this letter to analyze the linear optical property of the GNPs@MSTF nanocomposite.

The one-electron wave functions and the corresponding energy levels are shown as

$$\psi_{\rm hkl} = \left(\frac{8}{L^3}\right)^{1/2} \sin\left(\frac{h\pi x}{L}\right) \sin\left(\frac{k\pi y}{L}\right) \sin\left(\frac{l\pi z}{L}\right), \tag{1}$$

$$E_{\rm hkl} = \frac{\pi^2\hbar^2}{2mL^2}\left(h^2+k^2+l^2\right), \tag{2}$$

where L is the length of one edge of the potential well, and h, k, and l are positive integers. The dielectric function of the metal particle can be expressed as

$$\varepsilon_1 = \varepsilon_\infty + \frac{w_{\rm p}^2}{N}\sum_{i,f}\frac{s_{if}\left(F_i - F_f\right)}{w_{if}^2 - w^2 - iw\gamma_{if}}, \tag{3}$$

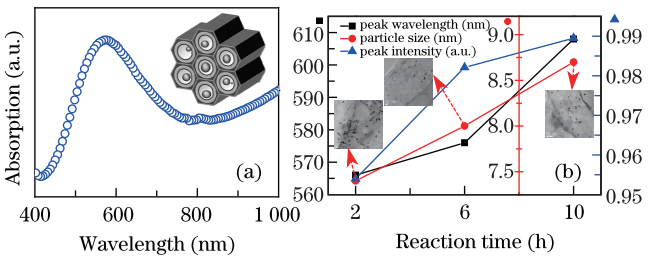

Fig. 3. (a) Experimental data of the absorption spectrum of a GNPs@MSTF composite film with six-hour reaction time; the inset is a model of the nanocomposite. (b) Experimental results of the absorption property of GNPs@MSTF composite films; the embedded TEM images show dispersed GNPs released from the nanocomposites with reaction time of 2, 6, and 10 h, respectively.

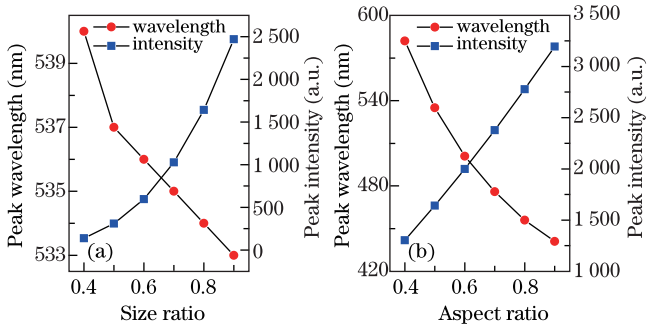

Fig. 4. Calculated results of the absorption peak location and intensity with varying (a) size ratio and (b) aspect ratio of GNPs; the calculations were done according to the model shown in the inset of Fig. 3(a).

where ε_∞ is the interband contribution to the dielectric function; w_p is the plasma frequency with $w_\mathrm{p}^2 = ne^2/(m\varepsilon_0)$, in which n is the concentration of electrons[11]; N is the number of electrons in the box of potential well; F_i and F_f are the values of the Fermi-Dirac distribution function for the initial and final states, respectively; s_{if}, w_{if}, and γ_{if} are the oscillator strength, the eigenfrequency, and the damping for the dipole transition from state i to f, respectively.

Under the restrictions of the dipole transitions[7], Eq. (3) can be written as

$$\varepsilon_1 = \varepsilon_\infty + w_\mathrm{p}^2 \sum_{\Delta l}^{1,3,\cdots} \sum_{l}^{l_\mathrm{F}} \frac{S_{l,\Delta l}}{w_{l,\Delta l}^2 - w^2 - iw\gamma_{l,\Delta l}}, \quad (4)$$

with

$$S_{l,\Delta l} = \frac{32}{\pi l_\mathrm{F}^3} \frac{l^2\,(l+\Delta l)^2}{\Delta l^2\,(2l+\Delta l)^2} \approx \frac{8}{\pi l_\mathrm{F}^3} \frac{l^2}{\Delta l^2}, \sum_{\Delta l} \sum_{l} S_{l,\Delta l} = 1, \quad (5)$$

where l_F is the value of intersection of the l-axis with the Fermi surface, which indicates the size of the particle and $l_\mathrm{F}^3 = N$, $n = l_\mathrm{F}^3/L^3$.

Along with the MG theory[12,13], the dielectric function of the solid thin film embedded with MNPs can be described as

$$\varepsilon_\mathrm{e}(w) = \varepsilon_2 \frac{\varepsilon_1\,(1+\kappa f_\mathrm{v}) + \kappa\varepsilon_2\,(1-f_\mathrm{v})}{(\varepsilon_1 + \kappa\varepsilon_2) - f_\mathrm{v}\,(\varepsilon_1 - \varepsilon_2)}, \quad (6)$$

where ε_2 is the dielectric constant of the matrix of the nanocomposite; f_v is the volume fraction of the particles; κ is the screen factor, and $\kappa = 2$ according to spherical particles. Then the extinction coefficient of the nanocomposite is obtained as

$$k(w) = \sqrt{\frac{1}{2}\left[\left(\mathrm{Re}^2(\varepsilon_\mathrm{e}) + \mathrm{Im}^2(\varepsilon_\mathrm{e})\right)^{1/2} - \mathrm{Re}(\varepsilon_\mathrm{e})\right]}. \quad (7)$$

Together with Eqs. (4), (6), and (7), we can obtain the extinction coefficient of the composite film. The calculated results are shown in Figs. 5(a)–(e). On the assumption that the volume fraction of GNPs is $f_\mathrm{v} = 0.01$, the values of l_F are 100, 50, 40, 30, and 20. As the radius of the gold atom is 144 pm, the corresponding lengths of the cubic GNPs are 28.8, 14.4, 11.52, 8.64, and 5.76 nm, respectively. On the assumption that the value of l_F is 30, the results were calculated, as shown in Figs. 5(A)–(E), when the volume fractions are 0.3, 0.2, 0.1, 0.01, and 0.001, respectively. In the calculation of the extinction coefficient, we adopt the following values[7]: $n = 5.9 \times 10^{28}$ m^{-3}, $w_\mathrm{p}/w_\mathrm{F} = 1.58$, $\varepsilon_2 = 3.9$, $\varepsilon_\infty = 4.0$, where w_F is the Fermi energy of the GNP. From the results of Fig. 5, we can draw a conclusion that the extinction peak moves to a longer wavelength when the sizes or volume fraction of the GNPs increase. In addition, many fine structures are observed in Fig. 5, providing evidence of the quantum size effects. However, it is difficult to see them experimentally as they are possibly covered up by the absorption spectra of the matrix and impurities on the film surface.

In the z-scan measurement, the beam waist at the focal plane was about 1 mm. The laser-supplying single pulses, which are centered at 720 nm with a pulse width of less than 100 fs, were focused onto the samples with a spot size of about 80 μm. The highest intensity was about 5.0 GW/cm^2 at the focal point. The aperture diameter was 20 mm, and the beam radius at the aperture was about 30 mm. The differences between the normalized valley and peak transmitted intensity are about 0.33, 0.32, 0.31, and 0.25 of curves a, b, c, and d in Fig. 6, respectively. The pre-focal transmittance valley followed by a post-focal transmittance peak implies the positive value of the refractive nonlinearity. According to the theoretical analyses made by Mansoor *et al.*[14], the nonlinear refractive index values of the sample prepared by P123 can be calculated to be about 1.14×10^{-10}, 1.11×10^{-10}, 1.07×10^{-10}, and 0.86×10^{-10} cm^2/W. Thereinto, curve b (Fig. 6) is a repeated measurement result of curve a, and curves c and d (Fig. 6) are the other two results measured at different places compared with curve a (or b). The coincidence of curves a and b (Fig. 6) indicates that there was no optical damage occurred during the measurement, and the effects of cumulative heating induced by the consecutive pulses did not exist. Moreover, on the femtosecond time scale of a pulse width, the thermal contribution to nonlinearity of the irradiated sample region induced by each single pulse can be ignored[15]. The

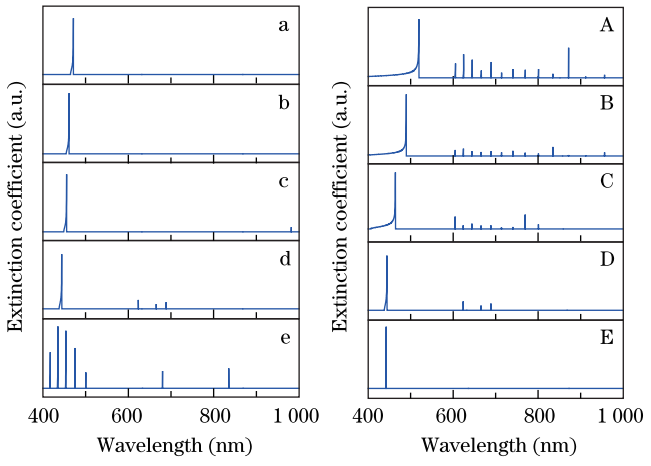

Fig. 5. Calculated extinction coefficients of GNPs in MSTFs with varying l_F (a: 100, b: 50, c: 40, d: 30, e: 20) and f_v (A: 0.3, B: 0.2, C: 0.1, D: 0.01, E: 0.001).

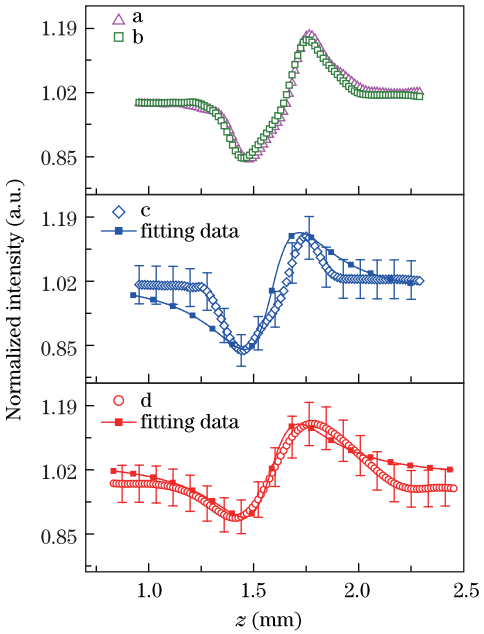

Fig. 6. z-scan trace of a GNPs@MSTF composite film with a six-hour reaction time: (a) and (b) are results of two measurements at the same place; (c) and (d) are the results of the other two different places; error bars are added with 5% of the error sources of data (c) and (d).

shapes of curves a, c, and d (Fig. 6) are qualitatively the same, implying that the nanocomposite possesses universal optic nonlinearity, whereas the differences between the index values suggest that the homogeneity of optic nonlinearity is not very good. The relatively wide size distribution (6.0–12.0 nm) and inhomogeneous GNPs loading in the pores (not every pore is loaded, and the loaded GNPs are not in the same pore depth) can seemingly account for this. Theoretical fittings were done to data c and d (Fig. 6). Although the valley and peak z coordinates are different between the experimental and analytical results, the valley–peak values determining the nonlinear refractive index values are within the bound of the ±5% error range. Moreover, nearly no interference structures of the transmission curves can be seen due to the vertical incidence of laser pulses.

In conclusion, the GNPs@MSTF nanocomposite film is prepared and its optical properties are studied. The linear optical absorption property is analyzed using a quantum mechanical model. The results show that the size and volume fraction of the GNPs will influence the peak location and intensity of the extinction spectrum. The nonlinear optical refractive index is measured by the z-scan technique, and the value is calculated to be about 10^{-10} cm^2/W.

This work was supported by the Advanced Research Foundation of the National University of Defense Technology (No. JC11-02-19) and the National Natural Science Foundation of China (No. 11104349).

References

1. H. Fan, K. Yang, D. M. Boye, T. Sigmon, K. J. Malloy, H. Xu, G. P. López, and C. J. Brinker, Science **304,** 567 (2004).
2. X. Zhang, Y. Chi, J. Fang, H. Zhong, S. Chang, L. Fang, and S. Qin, Phys. Lett. A **374,** 4880 (2010).
3. X. Zhang, W. Wu, J. Wang, and X. Tian, Appl. Surf. Sci. **254,** 2893 (2008).
4. J. Fang, X. Zhang, S. Qin, X. Li, F. Wang, and S. Chang, Chin. Sci. Bull. **56,** 728 (2011).
5. J. Fang, X. Zhang, S. Qin, and S. Chang, Chin. Opt. Lett. **9,** 032401 (2011).
6. J. Fang, S. Qin, S. Chang, and X. Zhang Microporous Mesoporous Mater **145,** 205 (2011).
7. L. Genzel, T. P. Martin, and U. Kreibig, Z. Physik B **21,** 339 (1975).
8. T. Xu, F. Chen, S. Dai, Q. Nie, X. Shen, and X. Wang, Chin. Opt. Lett. **8,** 70 (2010).
9. U. Kreibig, Appl. Phys. B **93,** 79 (2008).
10. A. Pinchuk, A. Hilge, and U. Kreibig, Surf. Sci. **557,** 269 (2004).
11. P. Mulvaney, Langmuir **12,** 788 (1996).
12. G. L. Hornyak, C. J. Patrissi, C. R. Martin, J.-C. Valmalette, J. Dutta, and H. Hofmann, Nanostruct. Mater. **9,** 575 (1997).
13. M. Y. Koledintseva, R. E. DuBroff, and R. W. Schwartz, PIER **63,** 223 (2006).
14. S.-B. Mansoor, A. A. Said, T.-H. Wei, D. J. Hagan, and E. W. Van Stryland, IEEE J. Quantum Electron. **26,** 760 (1990).
15. H. Liao, R. Xiao, H. Wang, K. S. Wong, and G. K. L. Wong, Appl. Phys. Lett. **72,** 1817 (1998).